JOURNAL OF MATERIALS SCIENCE 29 (1994) 73–79

Thermally stimulated discharge currents in corona-charged aramid paper

M. A. SUSSI, G. R. GOVINDA RAJU
Department of Electrical Engineering, University of Windsor, Windsor, Ontario, N9B 3P4, Canada

Thermally stimulated discharge (TSD) currents were measured in corona-charged aramid paper to study the mechanisms of charge storage and its subsequent release from the bulk of the material. Studies were carried out on paper thicknesses of 76 and 127 μm using a point-plane gap in air at atmospheric pressure. TSD currents were measured over a temperature range of 0–200 °C and the influence of various parameters, such as the poling voltage, rate of heating and effect of electrode materials, were investigated. Corona-charged aramid paper with positive polarity voltage showed that the TSD current is of either polarity depending upon the temperature range. Three distinct peaks were observed, one in the low-temperature range, 20–25 °C, and the other two peaks at higher temperatures. The low-temperature peak was considered to be due to an abnormal TSD current, whereas the currents at higher temperatures were normal TSD currents. Activation energies were determined using the low-temperature tail of the TSD curves and were found to be dependent on extrinsic parameters such as the thickness of the sample. The activation energy for aluminium electrodes was observed to be in the range of 0.5–2.0 eV. The TSD currents for the low-temperature peak was considered to be electronic. It is postulated that the charge carriers are generated within the material by the intense electric field due to corona.

1. Introduction

Measurement of thermally stimulated discharge (TSD) currents is a powerful technique that has been used to gain insight into the molecular mechanisms of charging of polymer dielectrics [1]. It also provides considerable information with regard to the relaxation processes that occur in polymers such as disorientation of dipoles and release of charges from trapping sites and impurity locations.

Several techniques are available for poling a dielectric material such as thermal, electron beam and corona poling. The latter consists of exposing the surface of the material to a corona discharge between point-plane electrodes with the point electrode being maintained at a high voltage. During measurement of the TSD currents, the polymer is heated linearly at a constant rate and a thermogram, which is a plot of current as a function of temperature, is obtained. The current shows a number of peaks to reveal processes which are related to molecular relaxation and delocalization of charges injected into the polymer bulk during poling [2–4].

In this paper the results of investigation into TSD currents of aramid paper (grade 410) using corona discharges are reported for the first time. Aramid paper, which is a high-temperature insulating material, has important industrial applications.

2. Theoretical background

We consider a polymer which is subjected to corona poling. Assuming a uniform charge density of free and trapped charge carriers, the charge in an element of thickness dx at a depth x and unit area is

$$dQ = \rho\, dx \tag{1}$$

in which ρ is the surface charge density. The contribution to the current in the external circuit due to release of this element of charge is [3]

$$dJ = \frac{W\,dQ}{s} = \frac{J(x)\,dx}{s} \tag{2}$$

where s is the thickness of the material, j the contribution to the externally measured current of the element of charge, W the velocity with which the charge layer moves, and $J(x)$ the local current due to the motion of the charge carriers.

According to Ohm's law, the current density is

$$J(x) = \rho\mu E(x) \tag{3}$$

where μ is the mobility and $E(x)$ the electric field at a depth x. The electric field is not uniform due to the presence of space charges within the material and it can be calculated by solving Poisson's equation

$$\frac{dE}{dx} = \frac{\rho_t}{\varepsilon_0 \varepsilon_r} \tag{4}$$

where ρ_t is the total charge density (free plus trapped) and ε_r is the dielectric constant of the material. If we denote the number of free and trapped charges by n_f

0022–2461

and n_t, respectively, the current density is

$$J = \frac{\mu e^2 \delta^2}{2\varepsilon_r s} n_f(n_f + n_t) \quad (5)$$

in which δ is the depth of the charge penetration, $\delta \ll x$ and e the electronic charge.

In general, it is reasonable to assume that $n_f \ll n_t$ and Equation 5 may be approximated to

$$J = \frac{\mu e^2 \delta^2}{2\varepsilon_r s} n_f n_t \quad (6)$$

The released charge carriers may be retrapped again and for the case of slow retrapping Creswell and Perlman [3, 4] have shown that

$$J = \frac{\mu e^2 \delta^2 n_{t0}^2}{2\varepsilon_0 \varepsilon_r s} \frac{\tau}{\tau_0} \exp\left[\left(-\frac{E_a}{kT} - \frac{2}{\beta\tau_0}\right) \times \int_{T_0}^{T} \exp\left(-\frac{E_a}{kT}\right) dT\right] \quad (7)$$

where n_{t0} is the initial density of charges in traps, τ the lifetime in traps, $1/\tau_0 = \nu$ the attempt to escape frequency, β the heating rate, E_a the trap depth below the conduction band, T, T_0 the final and initial temperatures respectively, of the TSD run (K), k is the Boltzmann constant, and

$$\tau = \tau_0 \exp\left(\frac{E_a}{kT}\right) \quad (8)$$

Equation 7 may be written in the form

$$J = A \exp\left[-p + \beta \int_{p_0}^{p} \exp(-p) p^{-2} dp\right] \quad (9)$$

where

$$A = \left(\frac{\mu e^2 \delta^2 n_{t0}^2}{2\varepsilon_0 \varepsilon_r s}\right) \frac{\tau}{\tau_0} \quad (10)$$

$$B = \frac{2E_a}{k\beta\tau_0} \quad (11)$$

$$p = E_a/kT \quad (12)$$

Differentiating Equation 9 and equating it to zero yields

$$B = p_{max}^2 \exp(p_{max}) \quad (13)$$

in which p_{max} is related to T_{max} according to Equation 12.

From the measured TSD currents, the activation energy may be calculated using the method suggested by Cowell and Woods [5] which is basically a curve-fitting method. All the measured values of current at various temperatures are used to obtain E_a to a better accuracy. An alternative method is to use the procedure suggested by Garlick and Gibson [6] in which $\ln j$ is plotted as a function of $1/T$ and the slope is evaluated by a least square error method.

The curves of current and temperature can also be used to evaluate the relaxation time of the material. The charge remaining in the sample at temperature, T, is given by

$$Q = \int_{t(T)}^{\infty} J \, dt \quad (14)$$

and the relaxation time at T is given by

$$\tau(T) = \frac{\int_{t(T)}^{\infty} J \, dt}{J(T)} = \frac{Q}{J(T)} \quad (15)$$

From Equation 8 the relaxation time is related to T according to

$$\ln\tau(T) = \ln\tau_0 + \frac{E_a}{kT} \quad (16)$$

A plot of $\ln\tau(T)$ versus $1/T$ yields E_a. It is useful to note that the current due to depolarization of permanent dipoles in the material results in an equation similar to Equation 7 except for the pre-exponential factor [7–9].

3. Experimental procedure

Aramid paper samples having a radius of 44 mm with thicknesses of 76 and 127 μm, were employed in this study. Prior to the experiments they were heated for 5 h at 260 °C to remove absorbed moisture. One side of the sample was coated with aluminium or silver electrode, 20 nm thick, by vapour deposition at a pressure of 10^{-6} torr. Following the coating, the sample was placed between a needle-shaped high-voltage electrode and a planar backing electrode. The gap length was 4.5 cm. For corona charging a potential of 16.83 kV or 33 kV was applied to the high-voltage electrode in air at atmospheric pressure for a period of 10 or 20 min. Fig. 1 shows a schematic illustration of the corona charging equipment. After charging a second aluminium electrode of the same thickness was vapour deposited on the other side. The sample was then placed between the measuring electrodes and kept short circuited for 1 h to remove any stray charges before it was cooled to 0 °C.

The TSD currents were measured by heating the sample at a constant rate of 2 K min^{-1}. An environmental chamber which was provided with a microprocessor was used to control the heating rate and the temperature range. The currents were recorded using

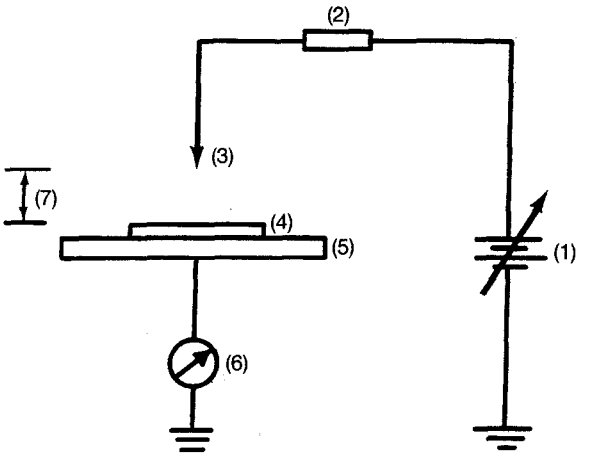

Figure 1 Schematic illustration of the corona-charging equipment. 1, Variable d.c. power supply; 2, current-limiting resistor; 3, point electrode; 4, sample; 5, current-measuring electrode; 6, electrometer; 7, gap distance (4.5 cm).

a Keithley electrometer and a strip chart recorder of 4 $\mu V\,mm^{-1}$ sensitivity.

4. Results and discussion

4.1. Influence of poling time and voltage

Fig. 2 shows the TSD currents in aramid paper for a thickness of 127 μm at a voltage of 16.83 and 33 kV. The negative polarity currents are normal TSD currents and the positive polarity currents are referred to as abnormal currents in this paper. In Fig. 2, the abnormal TSD currents flow in the circuit in the temperature range 0–40 °C, with a peak centred at 20–25 °C. Curve 1 which is obtained for a poling duration of 10 min at 16.83 kV, shows a peak in the normal TSD current at 62 °C. Increasing the poling duration to 20 min at the same voltage results in Curve 2 which shows two peaks, one at 72 °C and the other at 112 °C. A similar behaviour is observed for a higher voltage of 33 kV as shown by Curves 3 and 4. Similar results obtained for 76 μm paper are shown in Fig. 3 in which Curves 1 and 2 are for poling durations of 10 and 20 min, respectively.

Two observations are noted with regard to the effect of duration of poling. (i) As the poling duration increases, the low-temperature peak around 72 °C shifts to a higher temperature (Curves 3 and 4 of Fig. 2). (ii) The current magnitude at this peak is higher than that of the subsequent peak at about 110 °C. A similar behaviour is reported by Von-Seggern [10] and Sessler and West [11] for positive corona-charged Teflon and electron-injected FEP, respectively. The various peaks are assumed to be due to different trapping levels. As the poling time increases, the charges are trapped, possibly in deeper traps, and this will cause the peaks to shift to a higher temperature during release of charges.

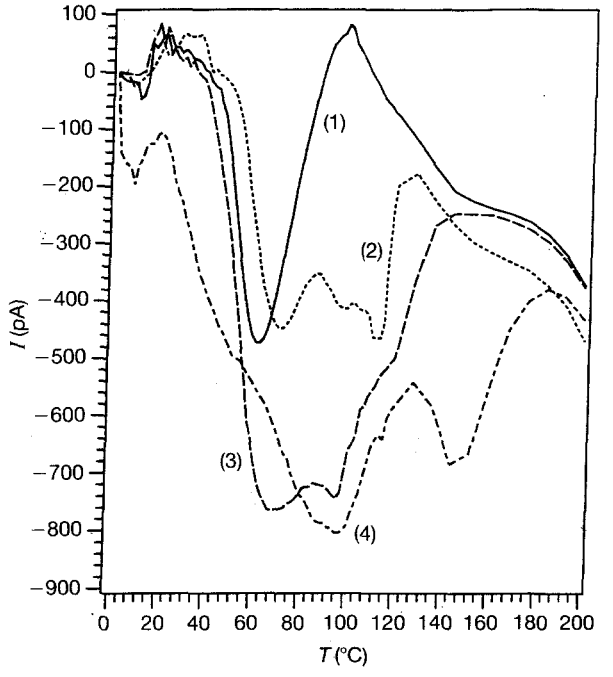

Figure 2 Thermally stimulated discharge (TSD) currents for positively charged 127 μm aromatic polyamide with aluminium electrodes. Charging voltage, charging time: (1) 16.83 kV, 10 min; (2) 16.83 kV, 20 min; (3) 33 kV, 10 min; (4) 33 kV, 20 min.

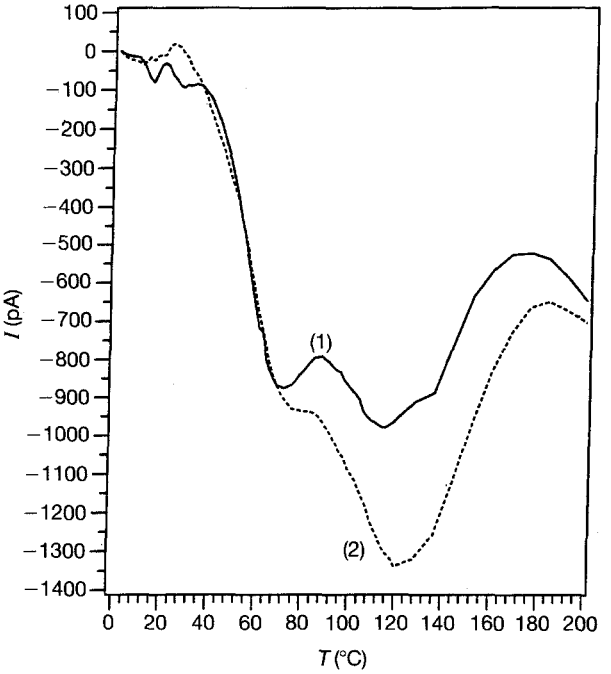

Figure 3 Thermally stimulated discharge (TSD) currents for positively charged 76 μm aromatic polyamide with aluminium electrodes. Charging voltage, charging time: (1) 16.83 kV, 10 min; (2) 16.83 kV, 20 min.

Fig. 2 also shows the influence of poling voltage on the TSD currents. The currents are higher for higher poling voltage. Furthermore, with increasing poling voltage the low-temperature peak at 72 °C becomes more pronounced (Curves 1 and 3 of Fig. 2) than those at higher temperatures. Neagu and Das Gupta [2] have observed a similar effect in Tefzel and suggest that the shallow trap density is probably greater than that for deeper traps.

The second peak in the normal TSD current occurs at 112 °C at 16.83 kV and shifts to 144 °C when the poling is increased to 33 kV. Sessler and West [11] have also observed a similar shift with electron-injected Teflon–FEP. They attributed the peak shift to the time dependence of radiation-induced conductivity generated during electron injection. The observed effect in aramid paper is probably ionic in nature, which is consistent with the fact that higher energy ions are generated in the discharge and they are trapped in deeper traps, as suggested earlier.

The calculated activation energies ranged from 0.5–0.98 eV for 76 μm and 0.5–2.0 eV for 127 μm samples and observed to be dependent on the poling voltages and independent of the poling time. Similar values of activation energies were reported in corona charged Mylar [3].

4.2. Influence of heating rate, β

The influence of rate of heating on TSD currents is shown in Fig. 4. These results are obtained with a thickness of 76 μm, Curves 1 and 2, and 127 μm, Curves 3 and 4, with aluminium electrodes for a time duration of 10 min and for a poling voltages of 33 and

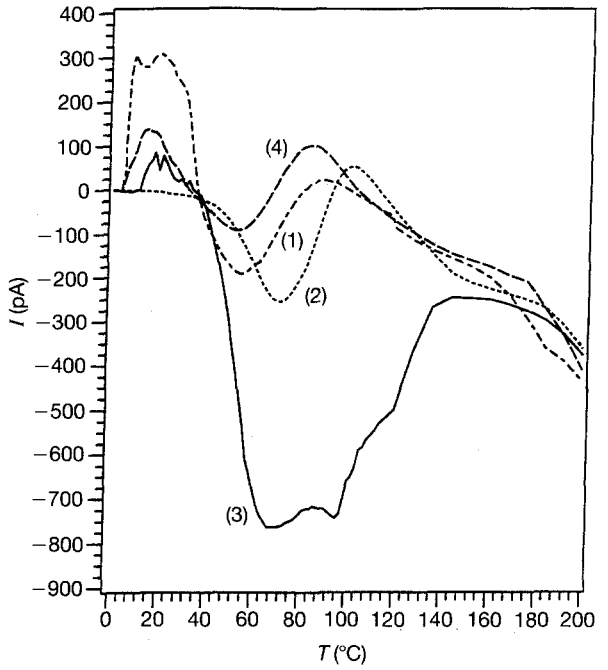

Figure 4 Influence of heating rates for 127 μm film with aluminium electrodes charged for 10 min. Charging voltage, heating rate, β: (1) 16.83 kV, 1; (2) 16.83 kV, 2; (3) 33 kV, 2; (4) 33 kV, 1.

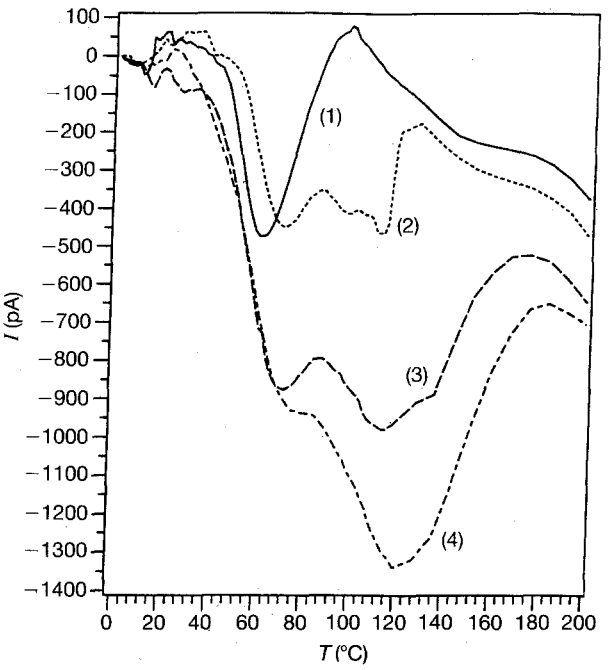

Figure 5 Influence of film thickness with aluminium electrodes charged with 16.83 kV. Charging time, paper thickness: (1) 10 min, 127 μm; (2) 20 min, 127 μm; (3) 10 min, 76 μm; (4) 20 min, 76 μm.

16.83 kV, respectively. The observed curves indicated that the current peak tends to shift to a lower temperature as β decreases. This is in general agreement with the theory [1] and the results of Creswell and Perlman [3] in corona-charged Mylar film. Fig. 4 also shows that a lower heating rate gives lower currents as expected.

The calculated activation energies were also found to be independent of the heating rate β. For instance, in Fig. 4, the activation energy obtained for Curves 1 and 2 at $\beta = 1$ and $2\,K\,min^{-1}$ is 0.75 eV for 16.85 kV, while for Curves 3 and 4 at the same values of β and 33 kV, the activation energy is 0.97 eV.

4.3. Influence of sample thickness

Fig. 5 shows the results obtained with two thicknesses for a poling duration of 20 min for Curves 2 and 4, and 10 min for Curves 1 and 3, at a poling voltage of 16.83 kV. The current magnitude is inversely proportional to the thickness of the film, thicker samples yielding lower currents with a higher activation energy of 2.0 eV. There is no appreciable dependence of the temperature at which the peak occurs on the sample thickness.

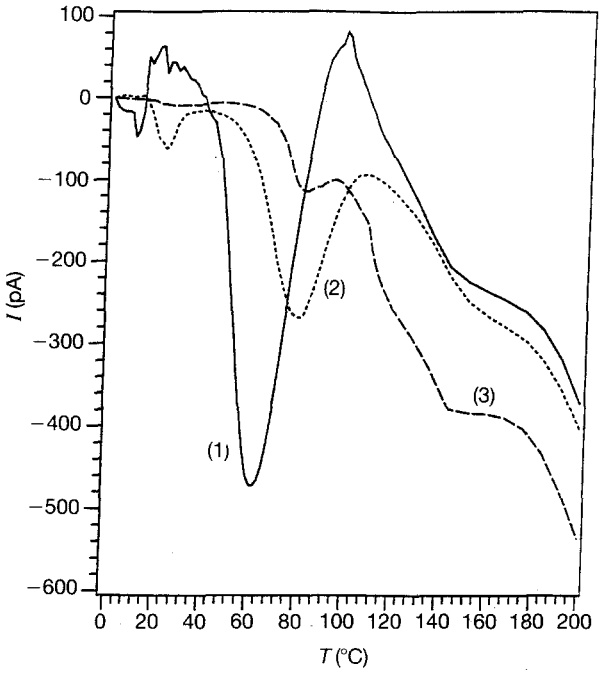

Figure 6 Influence of annealing time on TSD currents in aramid paper of 127 μm thick with aluminium electrodes charged with 16.84 kV. Heating time: (1) 1 h; (2) 6 h; (3) 48 h.

4.4. Influence of annealing time

The influence of annealing time on TSD currents is shown in Fig. 6. These results are obtained for aramid paper, with aluminium electrodes, having a thickness of 127 μm for a charging voltage of 16.83 kV and a poling duration of 10 min. The results are shown for annealing times of 1, 6 and 48 h. The peaks tends to shift to higher temperatures as the annealing time increases with decreasing magnitude. Similar results were reported by Sessler and West [11] for Teflon FEP charged with an electron beam, and the results were attributed to ohmic compensation of the primary electrons by secondary holes and the population shift depended on the total number of the holes available. The calculated activation energies were observed to be inversely dependent on the annealing time: the longer the annealing time, the lower the activation energy required to liberate the trapped charges. Curves 1–3 in Fig. 6 provide activation energies of 1.77, 0.94 and 0.56 eV for annealing times of 1, 6 and 48 h, respectively.

4.5. Influence of electrode materials

The influence of electrode materials on the TSD currents for a thickness of 76 μm film at a charging voltage of 16.83 kV are shown in Fig. 7. Curves 1 and 3 represent the TSD currents with aluminium electrodes at a poling time of 10 min while Curves 2 and 4 represent the TSD currents with silver electrodes. The results indicate that the TSD currents obtained with aluminium electrodes are much higher than those of the silver electrodes and it appears that the lower peak in Curves 1 and 3 (aluminium electrodes), disappeared in Curves 2 and 4 (silver electrodes). However, the position of the higher temperature peaks, in both materials, appears to be around the same temperature range of 90–120 °C. No results are available on other materials for comparison, because the effect of the electrode materials, in the case of corona charging, has not been discussed. However, in the case of aramid paper, the results indicated a dependency on the electrode materials, with silver electrodes showing some kind of blocking process.

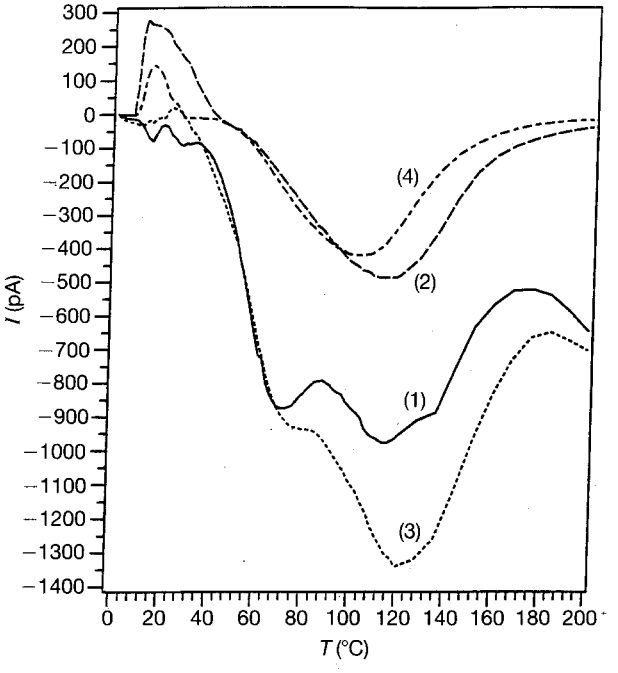

Figure 7 Influence of electrode materials on TSD currents for 76 μm paper charged with 16.83 kV. Charging time, electrode material: (1) 10 min, Al; (2) 10 min, Ag; (3) 20 min, Al; (4) 20 min, Ag.

4.6. Activation energy

The activation energy is determined for normal TSD current peaks at lower temperatures by using the initial rise method of Garlick and Gibson [6]. Typical values of activation energies obtained in this study from Fig. 8 are shown in Table I. No data are available for comparison. Sessler and West [12] found an activation energy in Teflon FEP in the range of 0.7–1.0 eV for the positive carrier peaks and 1.8 eV for the negative carrier peaks. However, Creswell and Perlman [3] reported several values of activation energies in positively corona charged Mylar of 0.55 and 0.85 eV to be due to electronic traps and 1.4 eV for either an electronic trap with a coulomb barrier, or an ionic trap. For a higher value of activation energy of 2.2 eV, the trap is identified to be either ionic, interfacial or involves dissociation of a complex with subsequent release of an electron to the conduction band. They also indicated that the transport during conduction is perhaps the only real distinguishing criterion. The activation energy obtained in this study for the low-temperature peak shows that the carriers are probably electronic. They are possibly generated with the bulk of the material by the intense radiation produced in the corona. They may also be generated by the intense electric field within the material during the charging process. Neagu and Das-Gupta [2] reported that with positive corona charging in air at atmospheric pressure, hydrated versions of H^+, NO^+ and NO_2^+ ions are produced, which could induce polarization in the polymer, whereas for negative corona charging, CO_3^- ions are generated. These ions may dissociate on the polymer surfaces to produce chemical changes in the polymer through the formation of double bonds and carbonyl groups [13].

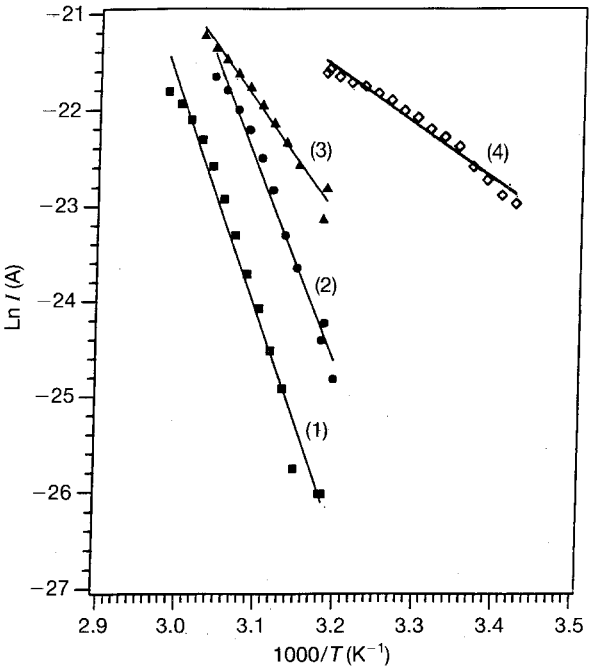

Figure 8 Influence of the charging voltage and charging time on the activation energy for 127 μm paper with aluminium electrodes. Charging voltage, charging time, activation energy: (1) 16.83 kV, 10 min, 1.77 eV; (2) 16.83 kV, 20 min, 1.99 eV; (3) 33 kV, 10 min, 0.98 eV; (4) 33 kV, 20 min, 0.49 eV.

Table I shows a summary of the results obtained. The activation energies presented in Table I were calculated for the first prominent peak in the normal TSD current thermogram. There is also a dependency on the poling time (i.e. charging time): in general, the longer the poling time the higher is the activation energy, as shown in Table I.

4.7. Relaxation time, τ

The relaxation time calculated in aramid paper (Equation 15) with thicknesses of 76 and 127 μm are shown in Fig. 9 for silver and aluminium electrodes. The

TABLE I Summary of results obtained from corona-charged aromatic polyamide paper

Charging voltage (kV)	Charging time (min)	Thickness (μm)	Electrode material	Temperature for maximum current T_m (°C)	Q (10^6 C)	E_a (eV)	Figure	Curve
16.83	10	76	Al	72,113.6	3.469	0.66	7	1
	20	76	Al	80,120	4.340	0.55	7	3
16.83	10	76	Ag	113.6	1.263	0.71	7	2
	20	76	Ag	104	0.906	0.82	7	4
16.83	10	127	Al	62.4	0.977	1.77	2	1
	20	127	Al	72,112	1.529	1.99	2	2
33	10	127	Al	70,496	2.183	0.98	2	3
	20	127	Al	96,144	3.012	0.49	2	4

TABLE II Typical values of the concentration of the charge carrier and its mobility with monomolecular and bimolecular recombination mechanisms from TSD current measurements

Figure	Curve	Monomolecular n_t (10^{18} m^{-3})	Bimolecular n_t (10^{18} m^{-3})	Monomolecular μ (cm^2 V^{-1} s^{-1})	Bimolecular μ (cm^2 V^{-1} s^{-1})
2	1	3.37	4.99	8.29	3.78
2	2	3.00	4.44	9.90	4.51
2	3	10.13	15.01	1.48	0.68
2	4	25.05	37.11	0.25	0.11
7	1	29.87	44.25	0.33	0.15
7	2	19.36	28.68	0.44	0.20
7	3	71.09	105.32	0.09	0.04
7	4	13.78	20.41	0.75	0.34

relaxation times obtained show a distribution in the bulk of the sample. A typical value of relaxation time for silver in the range of 40–192 °C is 11×10^5–120 s. For aluminium, τ ranges from 35×10^5–24 s in the range 38–86 °C.

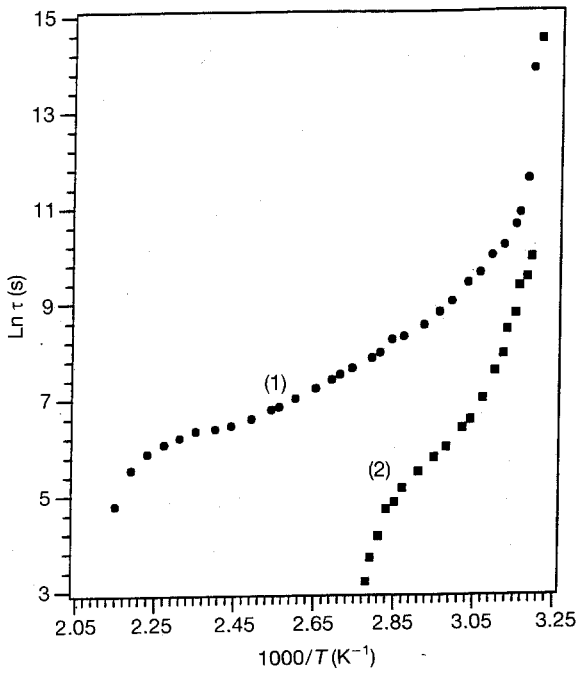

Figure 9 Plot of ln τ versus $1/T$ for samples charged at 16.83 kV for 10 min. Sample thickness, electrode material: (1) 76 μm, Ag; (2) 127 μm, Al.

4.8. Concentration of charge carriers, n_t

The total charge Q_t, released during the TSD current spectrum obtained, using Equation 4 is noted in Table I. Q_t was observed to increase with increasing poling time.

The concentration of charge carriers, n_t, captured by traps, for both cases of monomolecular and bimolecular recombination with weak and strong retrapping, is given by Bordowskii [14], for monomolecular retrapping

$$n_t = \frac{2.7 J_m k T_m^2}{eL\beta E_a} \quad (17)$$

where J_m is the maximum current density, T_m the temperature at which the maximum current occurs, and L the depth of the space charge layer.

In the case of strong bimolecular recombination, the above equation differs only by a factor of 1.48 higher [14]. Table II shows the values of n_t obtained in both cases.

The mobility of the charge can be calculated using Equation 6 and the derived values of n_t. The penetration depth of the space charge layer is assumed to be at mid-point of the sample thickness and n_f/n_t is assumed as 0.5. The mobility of the charge carriers calculated for the conditions listed in Table II are in agreement with those given elsewhere [15].

Two possible models have been suggested [15] for the charge-carrier transport in molecular crystals. The first model deals with the conventional band theory with mobilities greater than 1 cm^2 V^{-1} s^{-1} which vary as T^{-n}, where n is in the range of 1.5, and the second

deals with the hopping polaron model mobilities for which it is less than 1 $cm^2 V^{-1} s^{-1}$ and varies according to $\exp(-Ev/kT)$. Also, higher mobilities which lie between 1 and 100 $cm^2 V^{-1} s^{-1}$ and obey a T^{-n} temperature law have been reported in pure molecular crystals. Aramid paper is manufactured from aromatic polyamide in the form of fibres which are amorphous and flocs which are crystalline, the finished product having a crystallinity of approximately 50% [9]. An increasing mobility is thought to indicate an increasing predominance of the crystalline region in the conductor process.

4.9. Dipole moment, μ_p

The electrical dipole moment, μ_p, is calculated for Nomex 410 using the Debye Equation 18

$$\frac{\varepsilon_r - 1}{\varepsilon_r + 2} = \frac{N\mu_p^2}{9\varepsilon_0 kT} \tag{18}$$

where $\varepsilon_r = 2.5$ is the dielectric constant of the material, ε_0 the permittivity of free space, and N the number of monomers per cubic metre. The molecular weight is 242.3

With N_0 the Avogadro number, D the density ($kg\,m^{-3}$), and W the total molecular weight, and the density provided by the data sheet as 960 $kg\,m^{-3}$, the calculated number of monomers per unit volume obtained using Equation 19 is found to be $2.4 \times 10^{27}\ m^{-3}$

$$N = N_0 \times \frac{D}{W} \tag{19}$$

The dipole moment obtained from Equation 18 at $T = 335.5$ K is 8.377×10^{-30} Cm which is 2.5 Debye. To determine the bond to which the observed dipole moment may be attributed, values of the bond moment must be known. The reported values of the bond moment [16] for C–O, C–N, H–N, and H–C are 2.4, 0.4, 1.3 and 0.4 Debye, respectively. From these reported values, the C–O bond which has 2.4 Debye dipole moment and which is located in the side group, is most likely responsible for the obtained value of 2.5 Debye.

References

1. J. VAN TURNHOUT, in "electrets", edited by G. M. Sessler (Springer, Berlin, 1980).
2. E. NEAGU and D. K. DAS-GUPTA, *IEEE Trans. Electr. Insul.* **24** (1989) 489.
3. R. A. CRESWELL and M. M. PERLMAN, *J. Appl. Phys.* **41** (1970) 2365.
4. M. M. PERLMAN, *J. Electrochem. Soc: Solid State Sci. Technol.* **119** (1972) 892.
5. T. A. T. COWELL and J. WOODS, *Br. J. Appl. Phys.* **18** (1967) 1045.
6. G. F. J. GARLICK and A. F. GIBSON, *Proc. Phys. Soc.* **60** (1948) 574.
7. I. M. TALWAR and D. L. SHARMA, *J. Electrochem. Soc. Solid State Sci. Technol.* **125** (1978) 434.
8. G. R. GOVINDA RAJU, *IEEE Trans. Elect. Insul.* **27** (1992) 162.
9. M. A. SUSSI and G. R. GOVINDA RAJU, *SAMPE J.* August (1992) to be published.
10. H. VON SEGGERN, *J. Appl. Phys.* **52** (1981) 4081.
11. G. M. SESSLER and J. E. WEST, *Phys. Rev.* **10** (1974) 4488.
12. *Idem, J. Appl. Phys.* **47** (1976) 3480.
13. M. M. PERLMAN and S. UNGEK, *J. Phys. D Appl. Phys.* **5** (1972) 2115.
14. G. A. BORDOWSKII, *Phys. Status Solidi (a)* **29** (1975) K183.
15. D. A. SEANOR, in "Polymer Science", edited by A. D. Jenkins (North-Holland, 1972) Ch. 17, pp. 1217–20.
16. J. W. SMITH, "Handbook of Electrical Dipole Moment" (Butterworths Scientific, London, 1955) pp. 241–4.

Received 2 June 1992
and accepted 8 June 1993